

## Scanning tunneling microscopy on Ga/Si(100)

H. Sakama and A. Kawazu

*Department of Applied Physics, The University of Tokyo, 7-3-1 Hongo, Bunkyo-ku, Tokyo 113, Japan*

T. Sueyoshi, T. Sato, and M. Iwatsuki

*JEOL Ltd., 3-1-2 Musashino, Akishima-shi, Tokyo 196, Japan*

(Received 22 February 1996)

The Ga/Si(100) surface is investigated using scanning tunneling microscopy (STM), scanning tunneling spectroscopy (STS), and low-energy electron diffraction. Two distinct peaks are observed on the  $2\times 2$  Ga phase using STS, which are associated with one Ga unoccupied state and two Ga-Si occupied states, respectively. The latter peak is assigned to surface state bands observed using angle-resolved photoelectron spectroscopy [Surf. Sci. **242**, 277 (1991)]. Regular arrays of Ga clusters are observed in STM images for the  $8\times 1$ -Ga phase. The spacing between Ga cluster arrays is constant, whereas the spacing between the clusters along an array fluctuates. Adjacent arrays are out of phase in the direction perpendicular to the arrays. Steps are severely deformed by the formation of the  $8\times 1$ -Ga phase. The initial stage and second-layer growths of the  $8\times 1$ -Ga phase are observed. Ga clusters disrupt the  $2\times 2$ -Ga phase. [S0163-1829(96)05636-6]

### I. INTRODUCTION

It is generally believed that the surface phases induced by group-III metal atoms (Al, Ga, and In) are categorized into two groups. One group contains  $2\times n$  ( $n=2, 3$ , and  $5$ ) phases, and the other consists of the  $8\times 1$ -Ga,  $c(4\times 2n)$ -Al, and  $4\times 3$ -In phases. Investigations have mainly focused on the  $2\times 2$  phase, with the use of low-energy electron diffraction (LEED),<sup>1</sup> angle-resolved photoelectron spectroscopy (ARPES),<sup>2-5</sup> x-ray standing-wave measurements,<sup>6</sup> and total-energy calculations.<sup>7,8</sup> The so-called parallel dimer model is widely accepted as the structure of the  $2\times 2$  phase. It was demonstrated that the images obtained by scanning tunneling microscopy (STM) are consistent with the parallel dimer model. STM studies were performed by several groups.<sup>9-13</sup> However, to the authors' knowledge, no scanning tunneling spectroscopy (STS) studies have been carried out so far.

In general, the surface phases which belong to the second group are formed at higher deposition temperatures than those in the first group.<sup>14</sup> The nature of chemical bonds between group-III metal atoms and Si atoms differs considerably between the two groups.<sup>15</sup> The phases in the second group have larger unit cells. The surface structures observed using STM appeared to be clusterlike, unlike those in the  $2\times n$ -Al, In phases.<sup>16,17</sup> The intrastructures of these clusterlike features have not yet been clarified, because they are very complex in comparison with those of the  $2\times n$  phases. In the  $8\times 1$ -Ga phase, periodic arrangements of clusterlike features similar to those in  $c(4\times 2n)$ -Al and  $4\times 3$ -In phases were seen in the image, although the size and the shape of clusterlike features differ among three systems.<sup>11</sup> However, more detailed information is needed to understand the structure of the  $8\times 1$ -Ga phase.

In this work, we perform STM and STS studies on the Si(100) $2\times 2$ -Ga phase. Two major peaks are observed, one of which is successfully assigned to the surface bands observed using ARPES.<sup>2</sup> The  $8\times 1$ -Ga phase is also observed

using STM and LEED. The features of STM images are discussed in conjunction with LEED patterns.

### II. EXPERIMENT

The STM study is performed in an ultrahigh-vacuum (UHV) system placed on an air damper.<sup>18</sup> The base pressure is less than  $1\times 10^{-8}$  Pa. The pressure during Ga deposition is kept below  $2\times 10^{-8}$  Pa. *P*-type Si(100) wafers with a resistivity of about  $10\ \Omega\ \text{cm}$  are used as substrates. The substrate is resistively heated by passing current through it. The substrate temperature is measured with an infrared pyrometer. Prior to the experiments, the substrate is repeatedly heated to and held at  $1200\ ^\circ\text{C}$  for 20 s, followed by slow cooling to below  $750\ ^\circ\text{C}$ . After the heat treatment, the surface reveals well-ordered dimer structures with  $2\times 1$  and  $1\times 2$  domains. Ga is evaporated from a heated tantalum basket. A constant deposition rate is achieved by controlling dc power supplied to the basket.

### III. $2\times 2$ PHASE

A well-ordered  $2\times 2$  phase is formed on Si(100) with a coverage of 0.5 ML at  $250$ – $500\ ^\circ\text{C}$ .<sup>14</sup> A STM image of this surface is shown in Fig. 1(a). In the middle of the image, the sample bias is abruptly switched from  $-2.0$  to  $2.0$  V, whereby the registry relationship of protrusions at the opposite bias polarities is determined. In this image, Si dimer rows run in the  $[0-11]$  direction. Protrusions are aligned across the boundary of the bias switch in the Si dimer direction (perpendicular to dimer row). However, a  $\pi$  phase shift of protrusions occurs in the direction of Si dimer rows. A similar behavior was observed on  $2\times 2$ -Al.<sup>11</sup> This result is explained well by the parallel dimer model in which Ga dimers with directions parallel to those of Si dimers are located in troughs of Si dimer rows. The registry of protrusions with respect to Si dimer structures is schematically illustrated in Fig. 1(b). Protrusions seen at the positive and negative sample bias voltages [*A* and *B* in Fig. 1(b)] can be

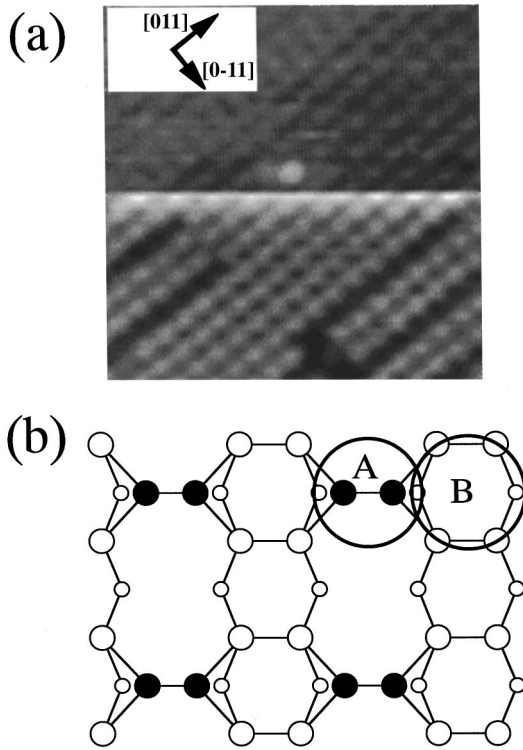


FIG. 1. (a) STM image of the  $2\times 2$ -Ga phase. The sample bias is switched from  $-2.0$  V (upper part) to  $2.0$  V (lower part) midway in the image. The tunneling current is  $1.0$  nA. Si dimer rows run in the  $[0-11]$  direction. (b) Schematic illustration of the parallel dimer model. Open and filled circles denote Si atoms and Ga atoms, respectively. Bold solid circles A and B show the locations of protrusions at positive and negative sample biases, respectively.

assigned to Ga and Si dimers, respectively.

STS measurements are performed on the  $2\times 2$ -Ga surface. Topographic images are taken at the sample bias of  $2.0$  V and tunneling current of  $1.0$  nA. The normalized conductivity is defined as  $(dI/dV)/(I/V)$ , which diverges at the surface band edge because  $I/V$  converges to zero faster than  $dI/dV$ . Thus the broadening of  $I/V$  by convolution with an exponential function is carried out with the broadening width of  $0.8$  eV.<sup>19</sup> The resultant normalized conductivity measured on the protrusions at positive and negative sample biases [A and B in Fig. 1(b)] are shown in Fig. 2. One characteristic peak is observed in Fig. 2(a). Apparently, this peak is due to Ga dimers. The STM images of  $2\times 2$ -Al at the positive (negative) sample bias were simulated using the local density of states (LDOS) of the unoccupied (occupied) states integrated around the bottom of the conduction band (the top of the valence band).<sup>8</sup> The protrusions seen at positive sample bias were assigned to the unoccupied dangling-bond states of Al. Thus the peak shown in Fig. 2(a) exhibits the LDOS of the unoccupied dangling-bond states of Ga. They have a maximum LDOS at  $1.44$  eV above the Fermi level ( $E_F$ ).

A broad peak is observed in Fig. 2(b) with a maximum intensity at  $1.80$  eV below  $E_F$ . The electronic structures of the  $2\times 2$ -Al,  $2\times 2$ -Ga, and  $2\times 2$ -In phases were investigated using ARPES.<sup>2-4,7</sup> Five bonding state bands were observed in the three systems. The shallowest band  $S_1$  has states with a binding energy of  $\sim 1.0$  eV.  $S_1$  is associated with Al (Ga,

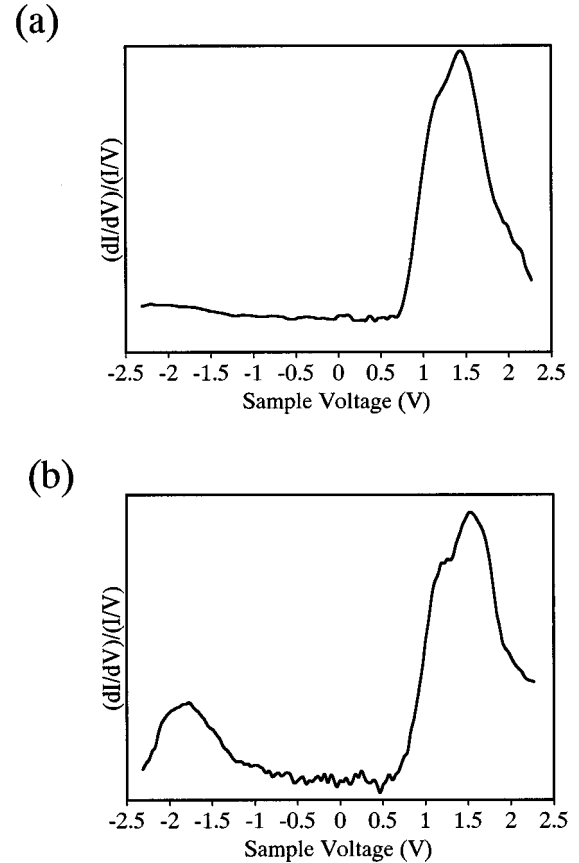


FIG. 2. STS spectra measured on (a) Ga dimers and (b) Si dimers. Topographic images are taken at a sample bias of  $2.0$  V and a tunneling current of  $1.0$  nA.

In) dimer bonds. Deeper bands, i.e.,  $S_2$  ( $S'_2$ ) and  $S_3$  ( $S'_3$ ), have states with binding energies of  $1.0$ – $1.5$  and  $1.5$ – $2.2$  eV, respectively. It was also shown that  $S_2$  ( $S'_2$ ) and  $S_3$  ( $S'_3$ ) are due to Al (Ga, In)-Si bonds. Therefore, the broad peak observed at  $1.80$  eV below  $E_F$  in Fig. 2(b) is successfully assigned to  $S_2$  ( $S'_2$ ) and  $S_3$  ( $S'_3$ ) bands obtained using ARPES.<sup>5</sup>

A very small peak observed at  $1.0$  eV below  $E_F$  may correspond to the  $S_1$  band. However, this  $S_1$  state has a maximum charge density between Ga dimer atoms and, therefore, has  $p_{xy}$  character (where the  $xy$  plane is parallel to the surface). The wave function of the  $S_1$  state must rapidly decay into the vacuum, which may be the reason for the smallness of the peak at  $1.0$  eV below  $E_F$ . Consequently, the STS spectra agree well with the ARPES results.<sup>5</sup>

On the clean Si(100)  $2\times 1$  surface,  $\pi$ -bonding states of Si dimers were observed with a binding energy of  $\sim 1.0$  eV.<sup>20</sup> The  $\sigma$ -bonding states of Si dimers and Si backbond states were shown to be located below  $E_F - 2.0$  eV. The dangling bonds on the clean surface are terminated, and the surface states associated with  $\pi$  bonds vanish by the formation of the  $2\times 2$ -Ga phase. Thus none of the surface states originating from the Si dimer structure were observed in STS spectra.

Another peak at the positive sample bias is identical to the peak seen in Fig. 2(a). Protrusions of Ga dimers are elongated in the Ga dimer direction, as shown in Fig. 1(a). Neighboring protrusions overlap at the boundary, which results in the existence of Ga dimer states above Si dimers.

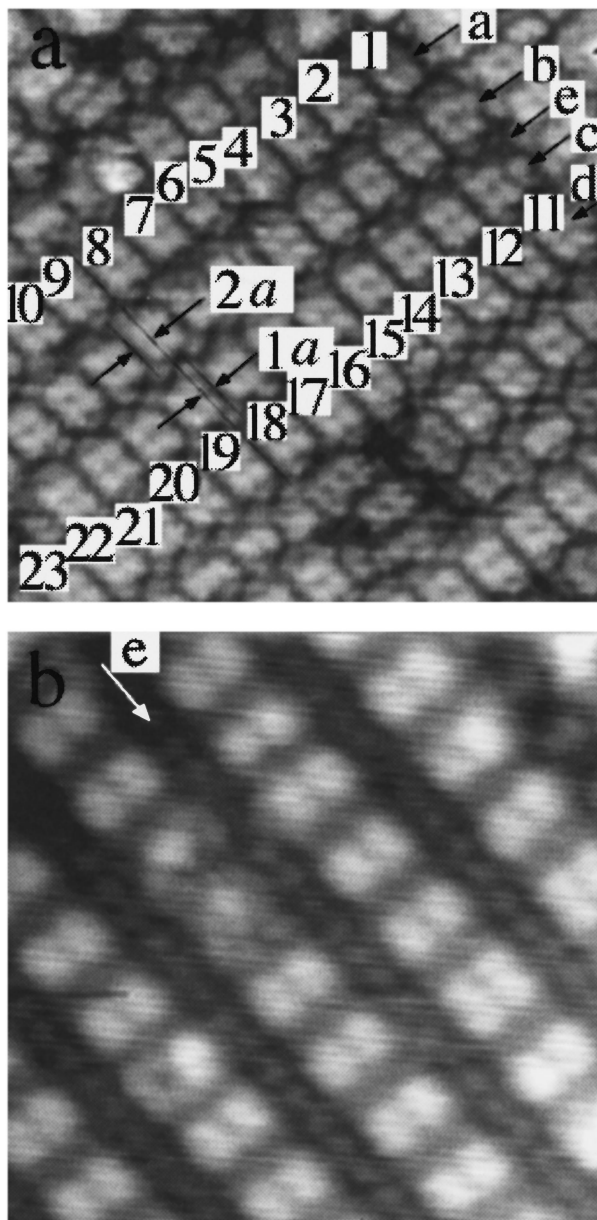


FIG. 3. STM image of the  $8 \times n$ -Ga phase with a coverage of 0.8 ML formed at  $450^\circ\text{C}$ : (a) sample bias  $-1.6\text{ V}$ , tunneling current  $0.2\text{ nA}$ ; (b) sample bias  $1.4\text{ V}$ , tunneling current  $0.2\text{ nA}$ . The directions of Si dimers on the predominant terraces are perpendicular to each other in (a) and (b).

#### IV. $8 \times n$ PHASE

Figure 3 shows STM images of the surface with a Ga coverage of 0.8 ML formed at  $450^\circ\text{C}$ . Regular arrays [e.g.,  $a-d$  in Fig. 3(a)] of rectangular clusters are observed. Similar clusters were observed in the  $c(4 \times 2n)$ -Al phase<sup>16</sup> and in the  $4 \times 3$ -In phase.<sup>17</sup> The common feature of these phases is that they are formed at elevated temperatures. The spacing between adjacent arrays is exactly  $8a$  [where  $a = 3.84\text{ \AA}$ , the period of the ideal Si(100) surface]. The predominant spacing along the array is  $5a$  between clusters labeled 1–23. However, the spacings between clusters 4–5–6 are  $3a$  and those between 6–7 and 13–14–15–16 are  $4a$ . Therefore, the surface phase should be referred to as  $8 \times n$ , with  $n = 3, 4$ , and

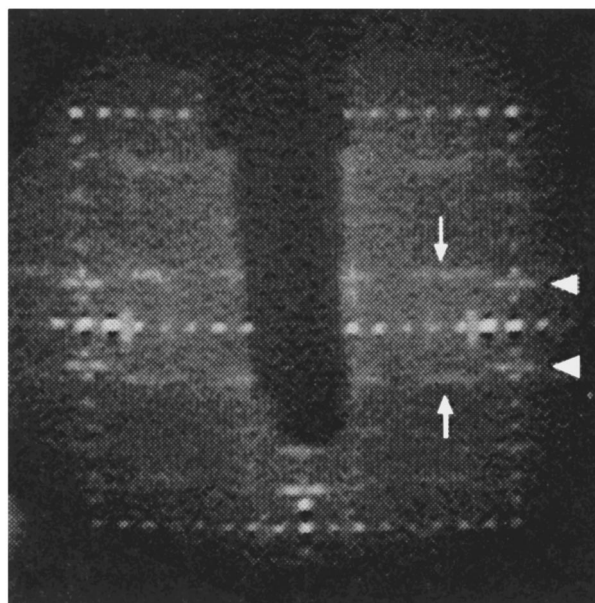


FIG. 4. LEED pattern from the  $8 \times n$  Ga phase.

5. This observation is consistent with that of the previous STM study by Baski, Nogami, and Quate, although they showed only  $n = 4$  and 5.<sup>11</sup> The size and shape of the clusters are almost identical. The clusters appeared to be oblong protrusions in the image given in the previous study.<sup>11</sup> Individual clusters are resolved into two subunits in the unoccupied state image [Fig. 3(b)], whereas they are resolved into four subunits in the occupied state image [Fig. 3(a)]. Small clusters (e.g., 5, 6, 14, and 15) can be seen in Fig. 3(a), which are responsible for the anomalous periodicity of  $n = 3$  and 4.

The adjacent arrays are frequently out of phase in the direction perpendicular to the arrays. For example, the arrays labeled  $b$  and  $c$  shift by  $2a$  and  $a$  in the opposite direction to the array labeled  $d$ , respectively. The LEED pattern from this surface only exhibits  $8 \times 1$  periodicity (Fig. 4). A similar LEED pattern was observed by Bouguignon, Carleton, and Leone.<sup>21</sup> We have already observed similar phenomena in Si(111) $5 \times 2$ -Au. In this system, the arrangements are ordered only along  $2 \times$  periodicity. One-dimensional rows along  $2 \times$  periodicity are out of phase with their neighbors along  $5 \times$  periodicity. The corresponding LEED pattern is  $5 \times 1$ .<sup>22</sup> According to the interpretation of the LEED pattern from Si(111) $5 \times 2$ -Au, the clusters shown in Fig. 3 lie on the regular  $8 \times 1$  lattices, though only one-fifth of these lattices are occupied on average.<sup>22</sup> This results in sharp spots corresponding to the  $8 \times 1$  pattern. In the Si(111) $5 \times 2$ -Au system, half-order streaks appear in the LEED pattern, which indicates  $2 \times$  periodicity. Continuous lines imply complete disorder along  $5 \times$  periodicity. Similar streaks are not observed in Fig. 4. Instead, spotty one-fifth-order diffraction features are observed, as indicated by arrowheads. These spotty features are reproduced in two-dimensional fast Fourier transform (2D FFT) patterns obtained from the STM images. Thus they are due to  $5 \times$  periodicity along the cluster arrays.

In the valley between adjacent cluster arrays, regular rows of protrusions are observed in Fig. 3(b) (e.g., that labeled  $e$ ). The spacing between protrusions is  $2a$ , which is similar to

the spacing between Ga dimers in  $2\times 2$ -Ga. However, these protrusions form zigzag chains along the rows in the occupied state image [labeled  $e$  in Fig. 3(a)]. Protrusions of zigzag chains shift by  $1.5a$  from their nearest neighbors in the direction perpendicular to the arrays. The spacing between equivalent protrusions along the rows is  $4a$ . Therefore, they do not correspond to Ga dimers. In the LEED pattern shown in Fig. 4, one-fourth-order streaks are observed, as indicated by arrows. From the 2D FFT patterns of STM images, they are shown to originate mainly from zigzag chains with  $4\times$  periodicity along the Ga cluster arrays.

The detailed atomic arrangement of the  $8\times n$  phase still remains unknown. Two models (dimerized structure model and incommensurate overlayer model) were proposed for the  $8\times n$  phase.<sup>21</sup> Ga atoms form dimers with one dimer missing every three dimers in the former model, while the Ga overlayer is formed incommensurately with underlying Si layers in the latter model. However, these two models appear to be inconsistent with the STM images. It was demonstrated that the desorption energy of Ga from Si(100) drastically decreases from the  $2\times 2$ -Ga phase (2.9 eV) to the  $8\times n$ -Ga phase (2.3 eV).<sup>15</sup> Moreover, dangling bonds on the clean surface are fully terminated by 0.5 ML of Ga, and the nature of bonding should be different in  $2\times 2$  and  $8\times n$  phases. Therefore, the formation of clusters shown in Fig. 3 is more natural than the formation of a two-dimensional Ga overlayer above 0.5 ML. An individual Al cluster is estimated to contain 5–6 Al atoms, and an individual In cluster is to contain 5–7 In atoms.<sup>13,17</sup> However, one Ga cluster should contain 32 Ga atoms when the surface is assumed to be completely covered with the  $8\times 5$  phase at 0.8 ML. This marked difference between Ga and Al, In cannot be explained so far.

Figure 5(a) shows a STM image of the surface with a Ga coverage of 0.5 ML formed at 450 °C. Almost the entire surface is covered with the  $2\times 2$  phase. However, bright protrusions are observed, which may be identical to the clusters shown in Fig. 3. The initial stage of cluster formation were also observed on Al-Si(100) and In-Si(100).<sup>16,17</sup> However, the difference among the three systems is that the clusters nucleate directly on the clean surface in  $c(4\times 2n)$ -Al and  $4\times 3$ -In, whereas the clusters grow after the completion of the  $2\times 2$ -Ga phase in  $8\times n$ -Ga. As indicated by an arrowhead in Fig. 5(a), extended dark areas are present in the vicinity of Ga clusters. This suggests that the growth of Ga clusters proceeds while disrupting the  $2\times 2$ -Ga phase.

The formation of Al and In clusters were considered to be accompanied by the displacement of underlying Si atoms.<sup>16,17</sup> This view was supported by the growth of a second Si layer on terraces at the initial stage of deposition.<sup>17</sup> Further evidence is that zigzag steps were formed with the completion of the  $c(4\times 2n)$ -Al phase, which was ascribed to trapping of displaced Si atoms at the original steps. Figure 5(b) shows an image from a surface with a Ga coverage slightly higher than that shown in Fig. 3. The surface is entirely covered with the  $8\times n$  phase. Zigzag steps similar to those on the Al-adsorbed surface are formed. Thus displacement of Si atoms and trapping of them at steps may occur during the growth of  $8\times n$ -Ga phase. A one-dimensional island indicated by an arrowhead is formed near the step edge on the upper terrace of the step. The clusters in this island are identical to Ga clusters in the  $8\times n$  phase. The direction of

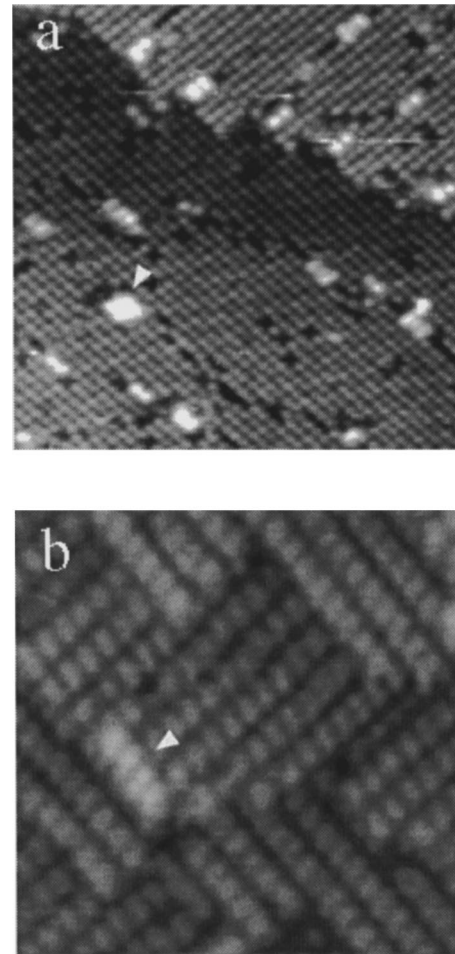


FIG. 5. (a) STM image of a Ga-adsorbed surface with a coverage of 0.5 ML formed at 450 °C. The sample bias is 2.0 V, and the tunneling current is 1.0 nA. (b) STM image of a Ga-adsorbed surface with a coverage slightly higher than that in Fig. 3. The sample bias is  $-1.6$  V, and the tunneling current is 0.2 nA.

the island is perpendicular to that of Ga cluster arrays on the same terrace. The number of such islands tends to increase with Ga coverage. Therefore, it seems that a second layer of the  $8\times n$  phase can be grown on the first layer.

## V. CONCLUSIONS

The Ga/Si(100) surface is investigated using STM, STS, and LEED. Protrusions seen at positive and negative sample bias voltages can be assigned to Ga and Si dimers. Two characteristic peaks are found using STS at 1.44 eV above and 1.80 eV below  $E_F$ . The latter peak is successfully assigned to the two occupied surface bands observed using ARPES.

Regular arrays of Ga clusters are observed with a constant spacing of  $8a$  between the arrays. The spacing between clusters along the array is  $na$  ( $n=3, 4, \text{ and } 5$ ). Adjacent arrays are out of phase in the direction perpendicular to the arrays, which is responsible for the  $8\times 1$  LEED pattern from the

$8 \times n$  phase. Additional features in the LEED pattern are well explained based on the STM images. The initial stage of cluster formation is also observed. The growth of Ga clusters proceeds while disrupting the  $2 \times 2$ -Ga phase. The deformation of steps is observed in the  $8 \times n$ -Ga phase. This is due to the displacement of Si atoms, and trapping of them at step edges during the formation of the  $8 \times n$ -Ga phase.

#### ACKNOWLEDGMENTS

We wish to thank Professor S. Kono and Dr. H. W. Yoem of Tohoku University for useful discussions. We also thank Dr. H. Shigekawa of Tsukuba University for valuable comments. This work was supported by a Grant-in-Aid for Science Research from the Ministry of Education, Science and Culture.

- 
- <sup>1</sup>H. Sakama, K. Murakami, K. Nishikata, and A. Kawazu, *Phys. Rev. B* **48**, 5278 (1993); **50**, 14 977 (1994); **53**, 1080 (1996).
- <sup>2</sup>Y. Enta, S. Suzuki, and S. Kono, *Surf. Sci.* **242**, 277 (1991).
- <sup>3</sup>H. W. Yoem, T. Abukawa, Y. Takakura, M. Nakamura, M. Kimura, A. Kakizaki, and S. Kono, *Surf. Sci.* **321**, L177 (1994).
- <sup>4</sup>H. W. Yoem, T. Abukawa, Y. Takakura, Y. Mori, T. Shimatani, A. Kakizaki, and S. Kono, *Phys. Rev. B* **53**, 1948 (1996).
- <sup>5</sup>H. W. Yoem (private communication).
- <sup>6</sup>S. Tang, A. J. Freeman, Y. Qian, G. E. Franklin, and M. J. Bedzyk, *Phys. Rev. B* **51**, 1593 (1995).
- <sup>7</sup>J. E. Northrup, M. C. Schabel, C. J. Karlsson, and R. I. G. Uhrberg, *Phys. Rev. B* **44**, 13 779 (1991).
- <sup>8</sup>G. Brocks and P. J. Kelly, *Phys. Rev. Lett.* **70**, 2786 (1993).
- <sup>9</sup>J. Nogami, S. Park, and C. F. Quate, *Appl. Phys. Lett.* **53**, 2086 (1988).
- <sup>10</sup>J. Nogami, A. A. Baski, and C. F. Quate, *J. Vac. Sci. Technol. A* **8**, 3520 (1990).
- <sup>11</sup>A. A. Baski, J. Nogami, and C. F. Quate, *J. Vac. Sci. Technol. A* **8**, 245 (1990).
- <sup>12</sup>J. Nogami, A. A. Baski, and C. F. Quate, *Phys. Rev. B* **44**, 1415 (1991).
- <sup>13</sup>H. Itoh, J. Itoh, A. Schmid, and T. Ichinokawa, *Phys. Rev. B* **48**, 14 663 (1993); *Surf. Sci.* **302**, 295 (1994).
- <sup>14</sup>K. Murakami, K. Nishikata, H. Sakama, and A. Kawazu (unpublished).
- <sup>15</sup>B. Bourguignon, R. Smilgys, and S. Leone, *Surf. Sci.* **204**, 473 (1988).
- <sup>16</sup>N. Shimizu, H. Kitada, and O. Ueda, *Phys. Rev. B* **51**, 5550 (1995).
- <sup>17</sup>A. A. Baski, J. Nogami, and C. F. Quate, *Phys. Rev. B* **43**, 9316 (1991).
- <sup>18</sup>H. Sakama, A. Kawazu, T. Sueyoshi, T. Sato, and M. Iwatsuki, *Jpn. J. Appl. Phys.* **32**, 2929 (1993).
- <sup>19</sup>P. Martensson and R. M. Feenstra, *Phys. Rev. B* **39**, 7744 (1989).
- <sup>20</sup>L. S. O. Johansson, R. I. G. Uhrberg, P. Martensson, and G. V. Hansson, *Phys. Rev. B* **42**, 1305 (1990).
- <sup>21</sup>B. Bourguignon, K. Carleton, and S. Leone, *Surf. Sci.* **204**, 455 (1988).
- <sup>22</sup>H. Lipson and K. E. Singer, *J. Phys. C* **7**, 12 (1974).